Available online at www.derpharmachemica.com

ISSN 0975-413X
CODEN (USA): PCHHAX

Der Pharma Chemica, 2017, 9(9):76-96
(http://www.derpharmachemica.com/archive.html)

Virtual Screening and Molecular Docking of 4,6,7-Tri Substituted Quinazoline Derivatives as Potential EGFR Inhibitors

Ahmad F Eweas[1,2], Owayyed M Al-Muqati[2], Rayid S Al-Osaimi[2], Mohammed D Al-Juaid[2]

[1]Department of Medicinal Chemistry, National Research Center, Dokki, Cairo, Egypt
[2]Department of Pharmaceutical Chemistry, College of Pharmacy, Taif University, Taif, Saudi Arabia

ABSTRACT

Despite the recent improvement achieved in cancer treatment strategies during the last three decades resulting in increasing the survival rate and better quality of life for cancer patients, cancer remains incurable in most cases. Search for new anti-cancer drugs is the subject of intensive research of many pharmaceutical companies and research centers. Molecular modeling simulation techniques are considered among the most modern methods to search for new drugs. In this research we decided to use molecular modeling and simulation of some derivatives 4, 6,7-trisubstituted Quinazolinones, known for their biological activities in various pharmacological uses especially as anti-tumor agents. The main idea in this work is to build a library of 90 compounds from 4,6,7-trisubstituted quinazoline family, and screen their binding affinity toward Epidermal Growth Factor (EGFR). The tested compounds are ranked according to their binding energy ΔG. The highest binding 10 compounds are analyzed in attempt to estimate their EGFR binding affinity using Molsoft ICM-Pro 3.5-0a software. The results reveled that most of the tested compounds have moderate to strong binding energy values in Kcal\mol towards EGFR target enzyme, which make them potential targets for drug discovery as new Tyrosine kinase EGFR inhibitors.

Keywords: 4,6,7-Trisubstituted quinazolines, Molecular docking, EFGR

INTRODUCTION

Drug discovery and development is an extremely expensive process because of the complicated technologies involved in the research and development stage in addition to the human clinical trials. The average overall cost per drug development lies between US$ 897 million and US$ 1.9 billion. The typical development time is 10-15 years [1]. The process starts with the discovery stage, which includes all early-stage research to identify a lead compound with potential lab testing results followed by lead optimization through altering its chemical structure to improve activity and pharmaceutical properties [2]. Based on average market data, this process takes approximately 3-6 years to complete the discovery stage. Molecular docking is a technique used in rational drug design in the early stage of drug discovery, which predicts the preferred orientation of one molecule to second, when bound to each other to form a stable complex [3].

Molecular docking aims to predict whether one molecule will bind to another. If the geometry of a pair of molecules is complementary and involves favorable biochemical and physical interactions, the two molecules will potentially bind *in vitro* or *in vivo* [4]. Current docking methodologies vary considering, e.g., Small molecules binding instead of macromolecular interactions, or rigid vs. flexible docking [5]. However, there are three common ingredients in docking:

A. Representation of the molecular structure: The structure of molecules first determined in laboratory relying on instrumental techniques as X-ray crystallography or Nuclear Magnetic Resonance (NMR) spectroscopy. Therefore, the basic description of a ligand surface is its atomic representation [6].
B. Conformational space search: The search space is all possible orientations and conformations of the interacting ligands. A search algorithm explores the search space to locate the most stable conformation. Each conformation of the paired molecules is referred to as a pose. Many strategies for sampling the search space are available in literature [7].
C. Ranking of possible solution: A scoring function computes the affinity between the receptor and the ligand.

Molecular docking algorithm screens large databases of molecules e.g. ZINC database orienting and scoring them in the binding site of a target protein. Top-ranked molecules are then tested for binding *in vitro*. Integrating pathways modelling with molecular docking enables researchers to incorporate experimental data on pathways with information on the structure of the compounds, and making more confident decisions on the future of the new drugs [8].

Unfortunately, algorithms and programs available differ for representation of the molecular structure, accuracy, computational costs, parameters, etc. [7].

In recent years, the heterocyclic fused nucleus quinazoline and their derivatives have drawn a great attention in the field of synthetic medicinal chemistry as they were reported to possess significant pharmacological activity [8-12]. Medicinally many substituted quinazoline derivatives are reported to possess a wide range of bioactivities as anti-malarial, anti-cancer, antimicrobial, antifungal, antiviral, anti-protozoan, anti-inflammatory, diuretic, muscle relaxant, antitubercular, CNS depressant, anti-convulsant, acaricidal, weedicide and many other functional materials [13].

Recently, 4,6,7-trisubstituted quinazoline derivatives started to draw attention for their potential biological activity specifically as Tumor Necrosis Factor-α (TNF-α) inhibitors [14], tyrosine kinase inhibitors [15] and inflammation modulator (IKKβ) inhibitors [16]. The clinical available Epidermal Growth Factor (EGFR) inhibitors, gefitinib, erlotinib and afatinib are all based on a 4-anilino-6,7- trisubstituted quinazoline core scaffold (Figure 1).

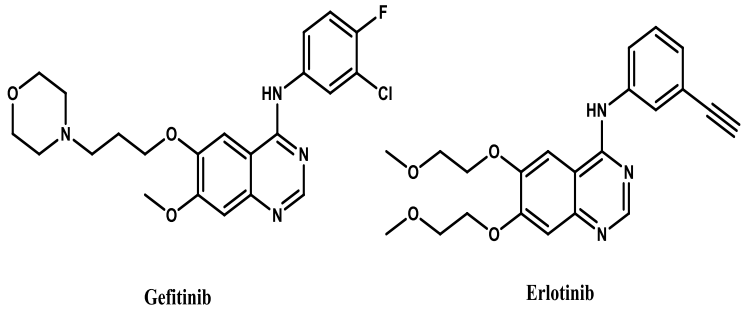

Gefitinib Erlotinib

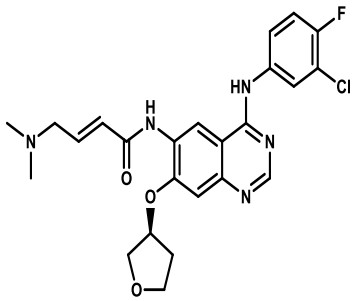

Afatinib

Figure 1: Quinazoline based EGFR-TK-selective inhibitors, gefitinib, erlotinib and afatinib

EGFR a group of protein tyrosine kinases (PTKs) is known for its role in cancer induction. Many of the tyrosine kinase enzymes are involved in cellular signaling pathways and regulate key cell functions such as proliferation, differentiation, anti-apoptotic signaling and neurite outgrowth [17]. Anilinoquinazolines are the most developed class of drugs that inhibit EGFR kinase intracellular. These compounds are being studied actively by many research groups and some of the drug candidates in this class have already reached various phases of clinical trials. Based on these findings, it seems rational to virtually screen a small library of new 4,6,7-trisubstituted quinazoline derivatives for their EGFR selectivity as potential anticancer agents using Molsoft-Pro (ICM 3.05a) docking software.

MATERIALS AND METHODS

Molecular modeling studies

All docking studies were performed using 'Internal Coordinate Mechanics (Molsoft ICM 3.5–aC).

Preparation of small molecule library

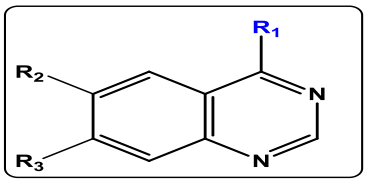

Figure 2: General structure of quinazoline tested compounds

A set of eighty nine 4,6,7-trisubstituted quinazoline derivatives (Tables 1 and 2), have been downloaded from the EGFRIndb database (http://crdd.osdd.net/raghava/egfrindb/). We used ChemDraw from (Chemoffice professional v 12) to compile them. 3D structures were constructed using Chem3D ultra 12.0 software [Molecular Modeling and Analysis; Cambridge Soft Corporation, USA (2010)] and then they were energetically minimized by using MOPAC (semi-empirical quantum mechanics), Job Type with 100 iterations and minimum RMS gradient of 0.01, and saved as MDL MolFile (*. mol).

Generation of ligand and enzyme structures

The crystal structure of the target protein, tyrosine kinase is an EGFR PDB id (1M17) enzyme complexed with Erlotinib was retrieved from the Protein Data Bank (www.rcsb.org/). All bound waters ligands and cofactors were removed from the protein.

Docking using Molsoft ICM 3.5-aC program

Convert the PDB file into an ICM object: This conversion involves addition of hydrogen bonds, assignment of atoms types, and charges from the residue templates.

To perform ICM small molecule docking

Setup docking project

(a) Set project name, (b) Setup the receptor, (c) Review and adjust binding site, (d) Make receptor maps. Start docking simulation.

Display the results

ICM stochastic global optimization algorithm attempts to find the global minimum of the energy function that include five grid potentials describing interaction of the flexible ligand with the receptor and internal conformational energy of the ligand, during this process a stack of alternative low energy conformations is saved (Table 2). The mode of interaction of the gefitinib within EGFR was used as a standard docked model. All inhibitors were compared according to the best binding free energy (minimum) obtained among all the run.

RESULTS AND DISCUSSION

The aim of the flexible docking calculations is the prediction of correct binding geometry of a small quinazoline derivative molecule and the target EGFR protein. The scoring functions and hydrogen bonds formed with the surrounding amino acids of the receptor EGFR are used to predict tested compounds binding modes. Gefitinib was used as reference drug for binding mode towards EGFR binding site. In this aspect a set of 89 compounds of 4,6,7-trisubstituted quinazoline derivatives of the general structure (Figure 2), was chosen for docking study against crystal structure of EGFR PDB id (1M17).

Docking and scoring of energy and hydrogen bonds formed with the surrounding amino acids of the receptor EGFR receptor using the docking program Molsoft ICM 3.5–a C between 89 compounds of qunizoline derivatives, substituted in position 4, 6 and 7 (Figure 1) was compared to FDA approved anticancer qunizoline (gefitinib). Molecular modeling of all compounds using ChemDraw 3D structures were constructed using Chem 3D ultra 12.0 software. All bound agents and waters were removed from EGFR crystal structure. Gefitinib the reference drug showed a binding energy of -85.44 Kcal/mol forming five hydrogen bonds with EGFR amino acid residues. On the other hand, docking results of all tested compounds towards EGFR crystal structure reveal moderate to high affinity ranging from -47.88-112.81 Kcal/mol.

The docking results of all tested compounds (Table 1) revealed that, all compounds under investigation showed moderate to high affinity ranging from -47.88-112.81 Kcal/mol. Because of the structural variations of the trisubstituted quinazoline compounds at the three variant positions 4, 6 and 7 quinazoline numbering. The tested compounds bind to different locations of the binding site of the target enzyme EGFR, forming hydrogen bonding with different amino acids in the binding site. A closer look at the results of the highest 10 compounds in the binding energy ΔG to the target enzyme. Namely compounds Qz47, Qz60, Qz66, Qz69, Qz72, Qz74, Qz83, Qz85, Qz86 and Qz89 (Table 2). A general structure binding relationship analysis can be drawing as following (Figure 3).

When the substituent in position 4 is a substituted N-anilino ring, the binding affinity of the quinazoline derivatives increases dramatically, mostly because of the ability of the NH group of the aniline ring to from hydrogen bond with the amino acid terminal of the EGFR binding site. In addition, the phenyl ring contributes to the binding affinity towards EGFR binding site through hydrophobic interactions. Furthermore, the substituent in position 6 seems to score high binding energy when it possesses aliphatic substituted Amido group (NH-CO-), obviously because of the hydrogen bonding formation ability of both NH and carbonyl group as hydrogen donor and acceptor groups. On the other hand, the substituents in position 7 scores high binding energy when having O- substituted aliphatic groups with small N or O five membered heterocyclic ring, which is structural similarity to the standard drug gefitinib. In general, most of the tested compounds scores high binding energy towards the target enzyme EGFR, which make 4,6,7-trisubtitued quinazoline an important scaffold for tyrosine kinase inhibitor anti-cancer drugs. Already among these compounds, there are marketed anti-colorectal cancer drugs like the itnib family including gefitinib, erlotinib and lapatinib.

Table 1: Docking results of substituted quinazoline derivatives against EGFR crystal structure

Compound number	R1	R2	R3	Docking score (Kcal/mol
Gefitinib	-	-	-	
Qz1	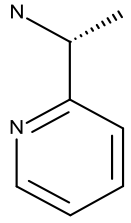	O-Me	O-Me	-89.90

Qz2	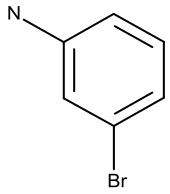	O-Me	O-Me	-52.34
Qz3	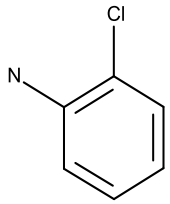	O-Me	O-Me	-77.26
Qz4	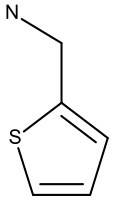	O-Me	O-Me	-94.00
Qz5	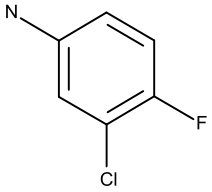	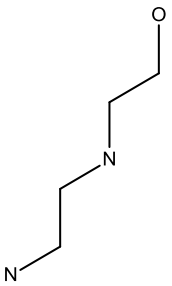	O-Me	-74.86
Qz6	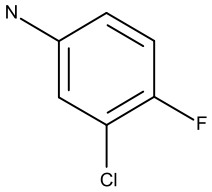	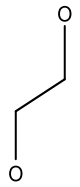	O-Me	-79.29
Qz7	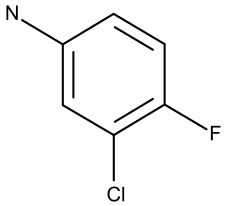	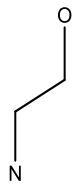	O-Me	-79.15
Qz8	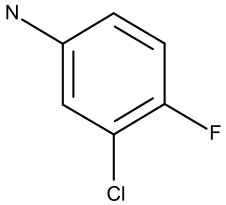	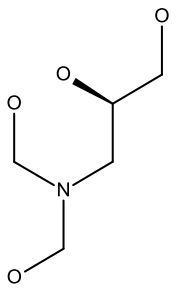	O-Me	-80.47

Qz9	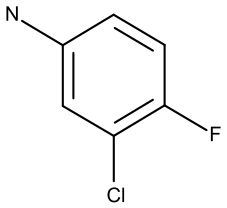	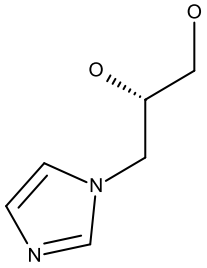	O-Me	-90.07
Qz10	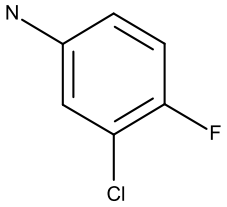	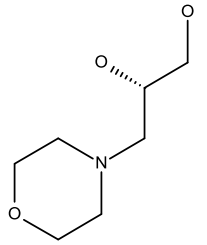	O-Me	-78.78
Qz11	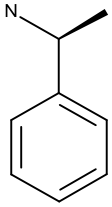	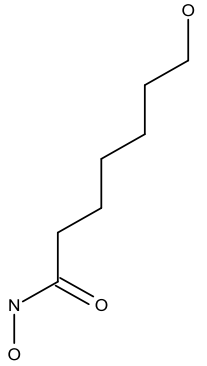	O-Me	-72.99
Qz12	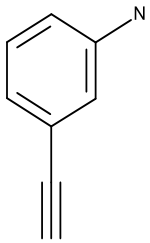	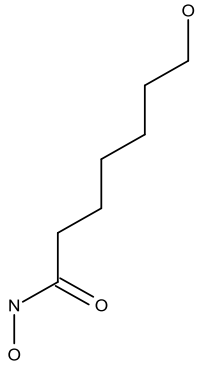	O-Me	-62.21
Qz13	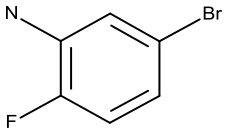	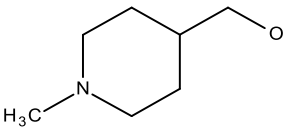	O-Me	-75.03
Qz14	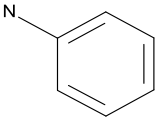	O-Me	O-Me	-66.73
Qz15	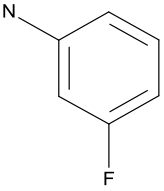	O-Me	O-Me	-52.96

Qz16	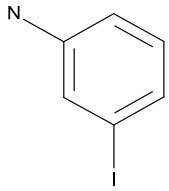	O-Me	O-Me	-59.30
Qz17	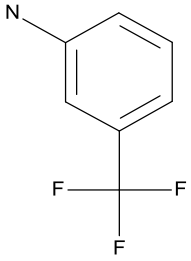	O-Me	O-Me	-73.28
Qz18	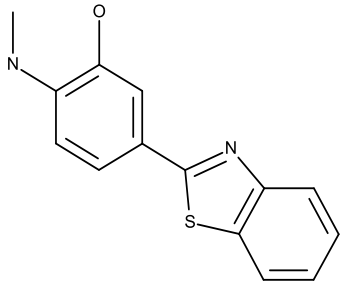	O-Me	O-Me	-72.75
Qz19	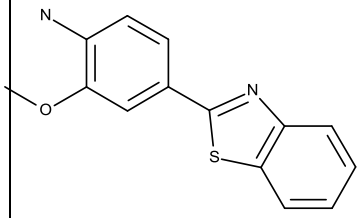	O-Me	O-Me	-72.56
Qz20	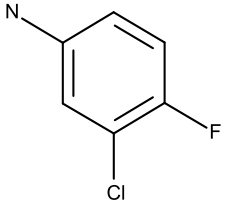	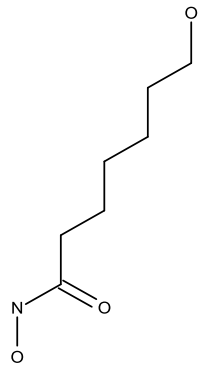	O-Me	-88.73
Qz21	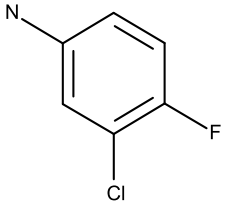	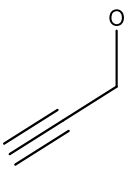	O-Me	-73.56

Qz22	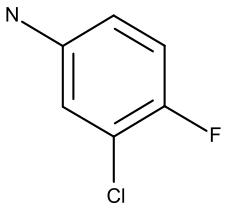	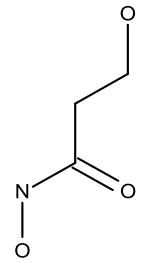	O-Me	-71.42
Qz23	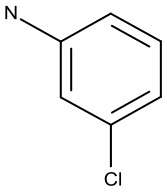	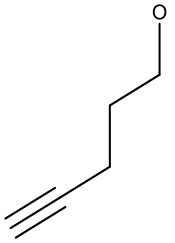	O-Me	-65.39
Qz24	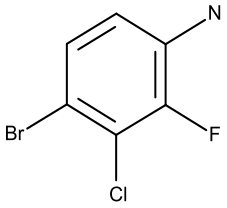	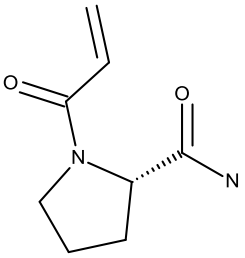	O-Me	-81.17
Qz25	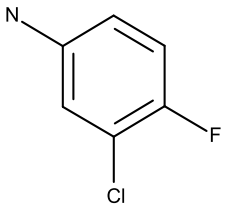	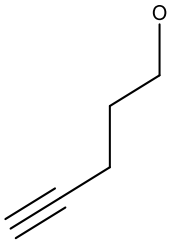	O-Me	-66.65
Qz26	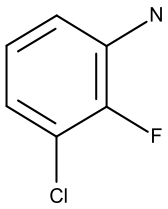	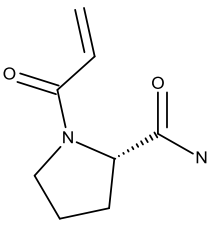	O-Me	-47.88
Qz27	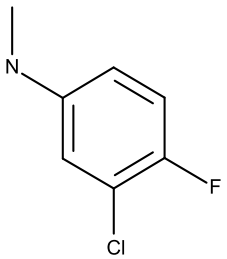	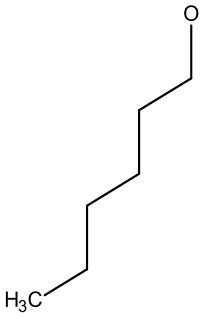	O-Me	-74.96

Qz28	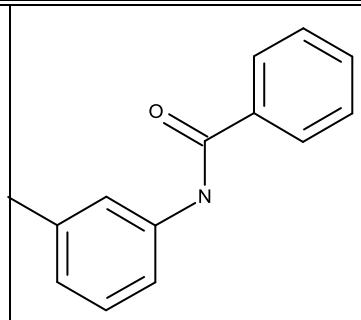	O-Me	O-Me	-83.53
Qz29	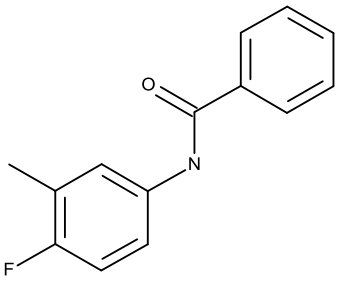	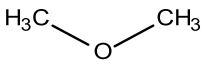	O-Me	-83.59
Qz30	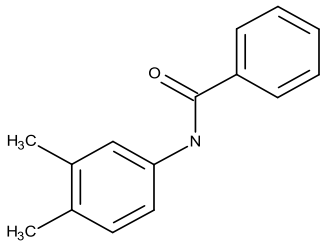	O-Me	O-Me	-79.02
Qz31	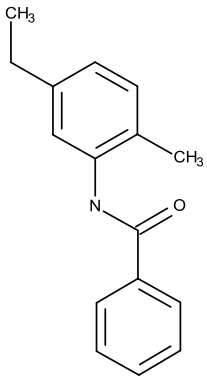	O-Me	O-Me	-85.89
Qz32	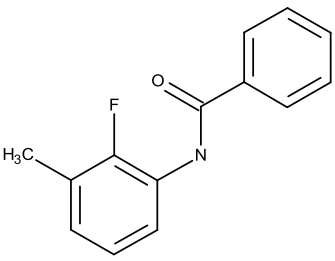	O-Me	O-Me	-78.73
Qz33	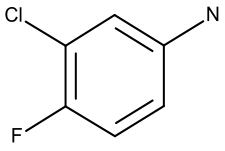	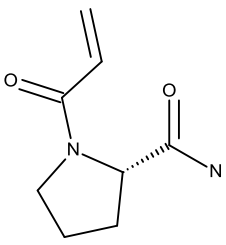	O-Me	-74.13

Qz34	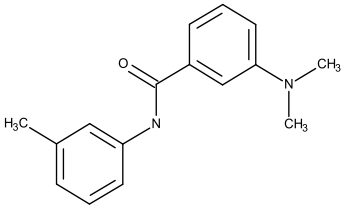	O-Me	O-Me	-84.49
Qz35	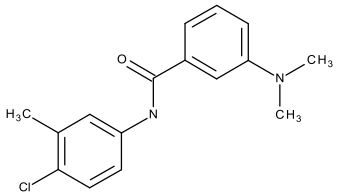	O-Me	O-Me	-84.95
Qz36	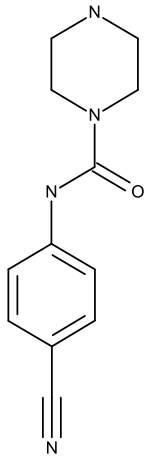	O-Me	O-Me	-94.64
Qz37	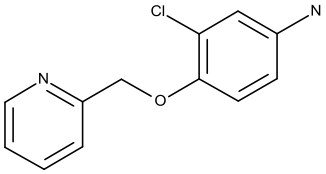	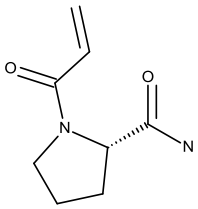	O-Me	-81.00
Qz38	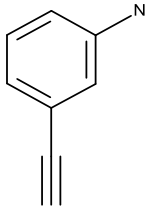	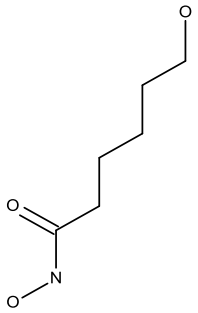	O-Me	-86.76

Qz39	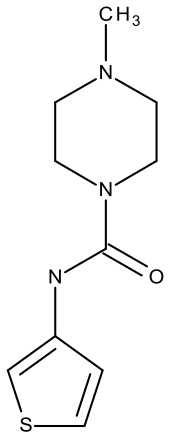	O-Me	O-Me	-86.80
Qz40	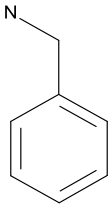	OH	O-Me	-78.10
Qz41	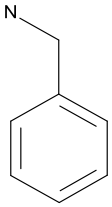	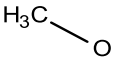	O-Me	-61.76
Qz42	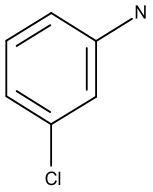	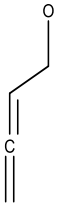	O-Me	-90.59
Qz43	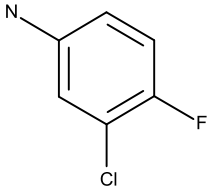	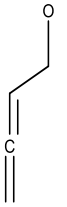	O-Me	-63.12
Qz44	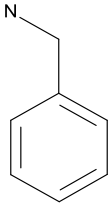	O-Me	OH	-70.97
Qz45	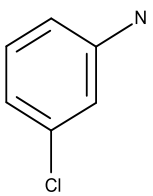	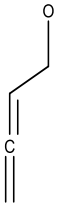	OH	-76.92

Qz46	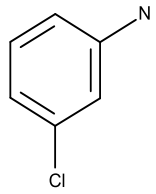	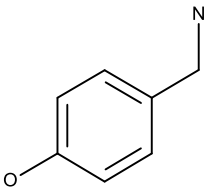	H	-97.14
Qz47	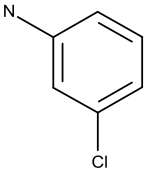	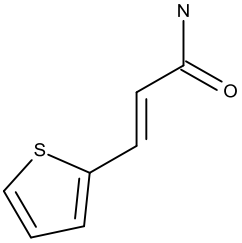	H	-74.10
Qz48	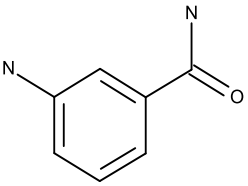	CH_3	H	-66.14
Qz49	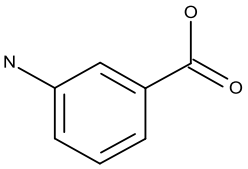	CH_3	H	-80.51
Qz50	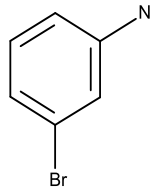	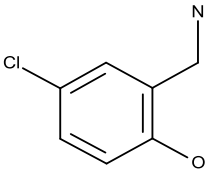	H	-72.19
Qz51	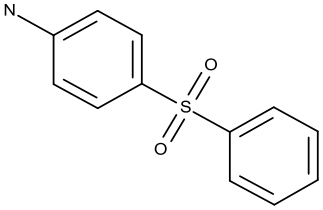	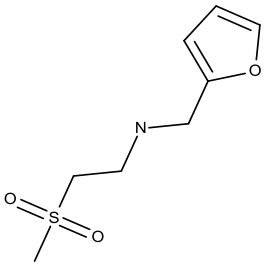	H	-74.91
Qz52	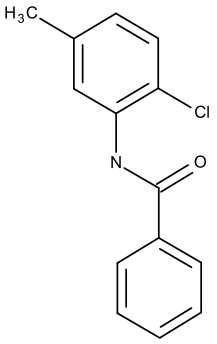	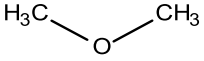	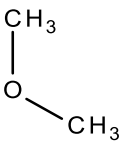	-72.02
Qz53	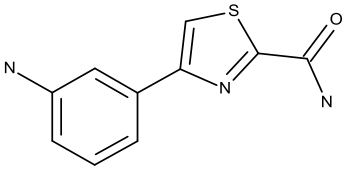	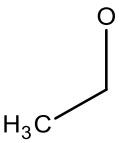	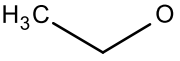	-84.91

Qz54	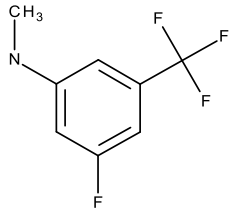	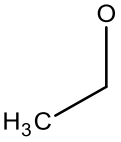	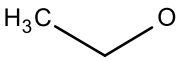	-63.55
Qz55	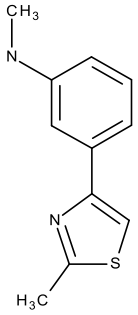	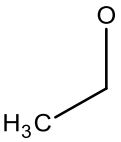	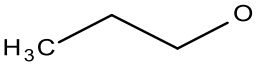	-77.01
Qz56	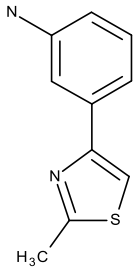	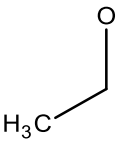	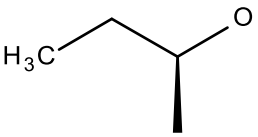	-63.42
Qz57	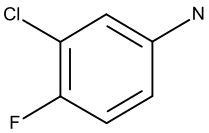	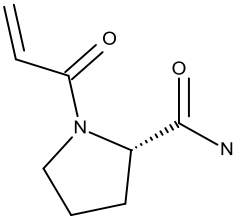	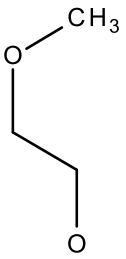	-81.78
Qz58	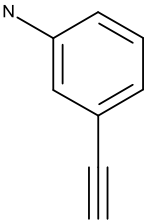	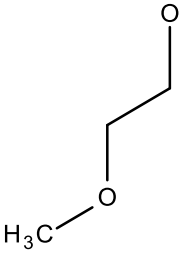	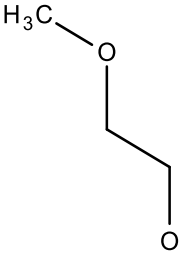	-62.20
Qz59	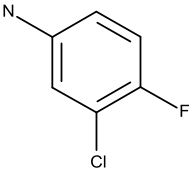	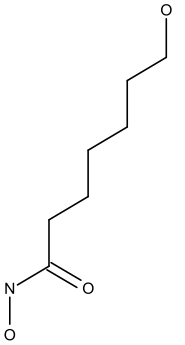	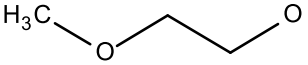	-112.09

Qz60	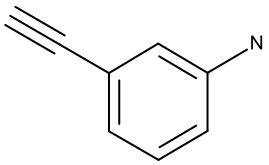	O-Me	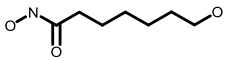	-63.68
Qz61	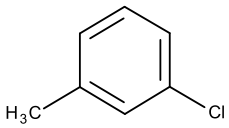	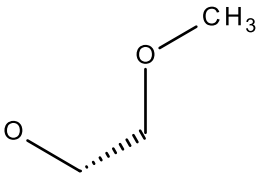	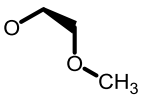	-79.56
Qz62	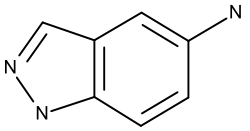	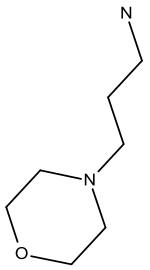	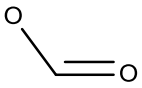	-87.00
Qz63	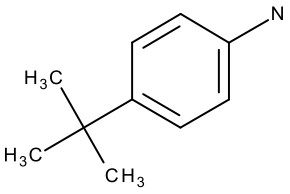	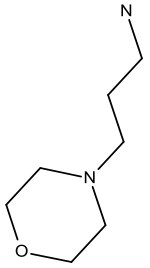	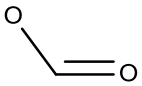	-95.34
Qz64	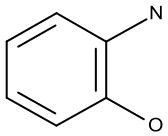	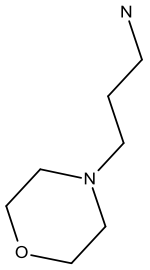	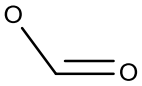	-84.60
Qz65	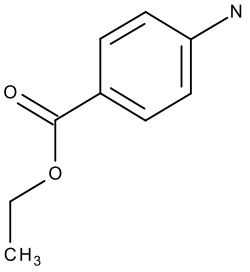	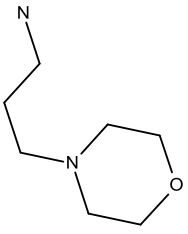	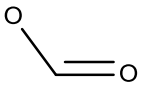	-102.02
Qz66	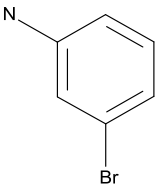	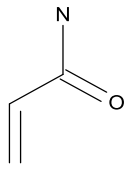	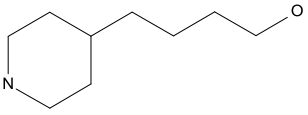	-64.70

Qz67	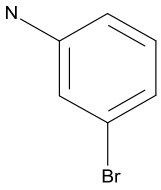	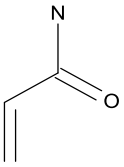	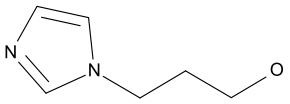	-85.10
Qz68	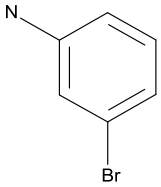	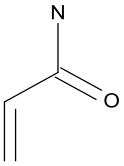	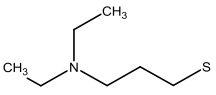	-109.64
Qz69	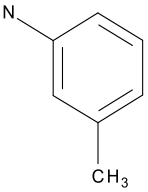	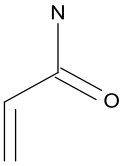	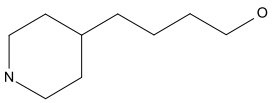	-82.28
Qz70	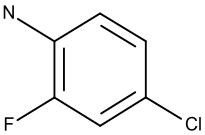	O-Me	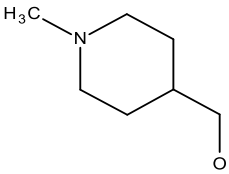	-87.43
Qz71	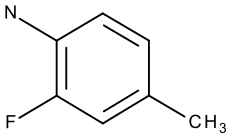	O-Me	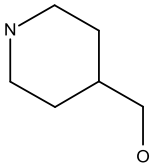	-112.81
Qz72	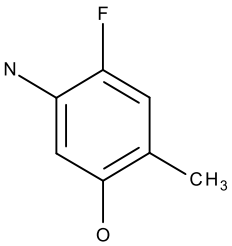	O-Me	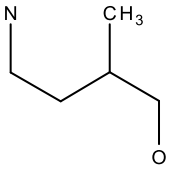	-85.18
Qz73	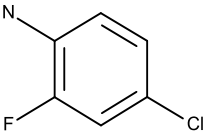	O-Me	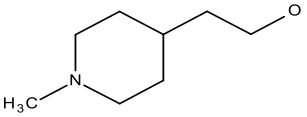	-106.77
Qz74	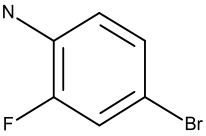	O-Me	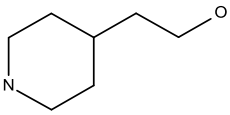	-72.71
Qz75	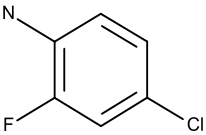	O-Me	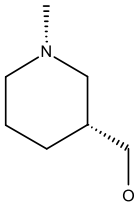	-96.41

Qz76	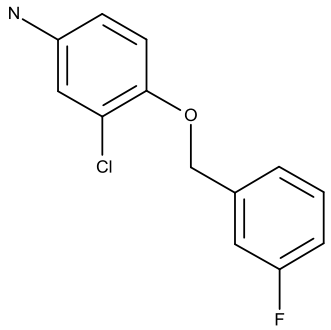	H	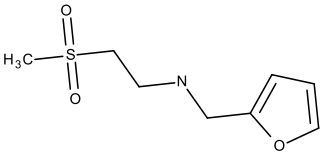	-77.71
Qz77	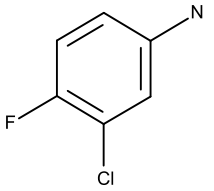	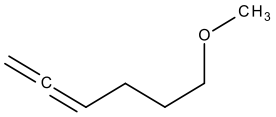	OH	-81.22
Qz78	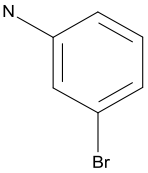	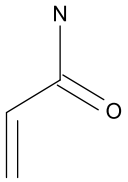	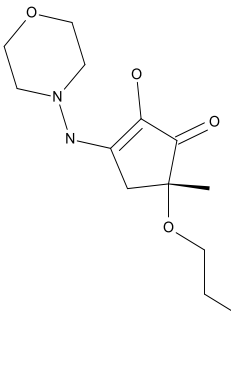	-75.22
Qz79	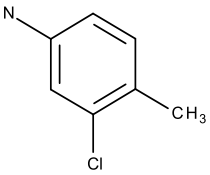	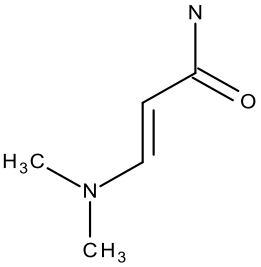	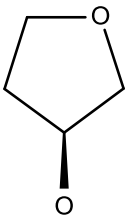	-73.89
Qz80	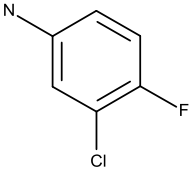	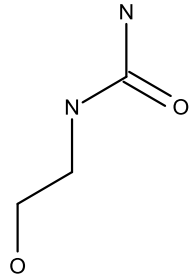	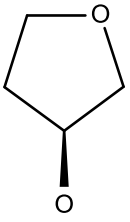	-85.51
Qz81	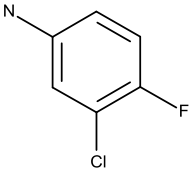	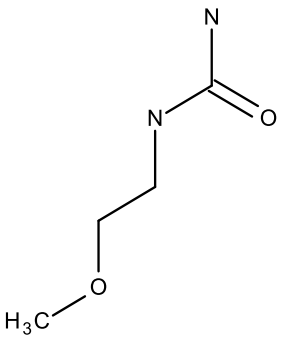	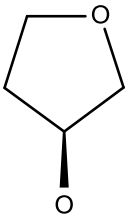	-89.25

Qz82	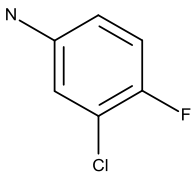	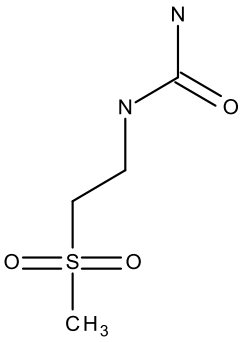	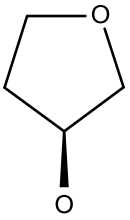	-104.78
Qz83	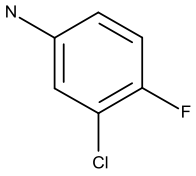	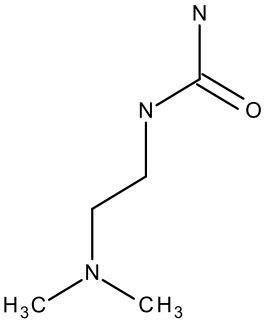	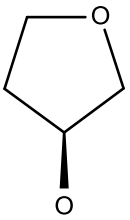	-91.15
Qz84	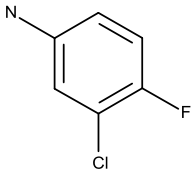	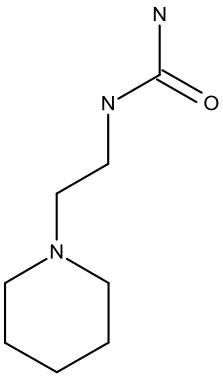	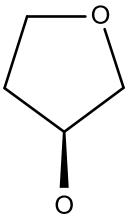	-109.78
Qz85	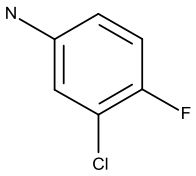	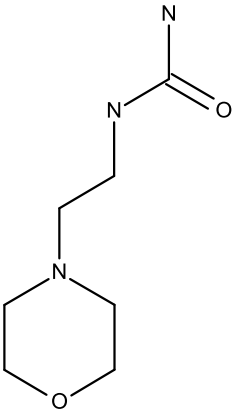	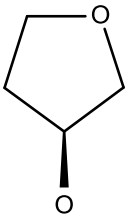	-100.03
Qz86	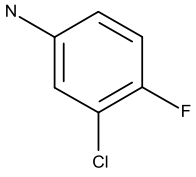	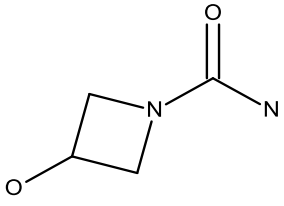	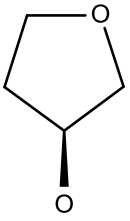	-94.07

Qz87	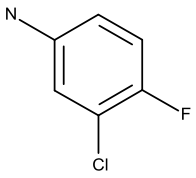	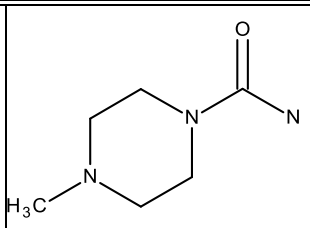	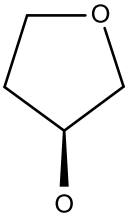	-83.21
Qz88	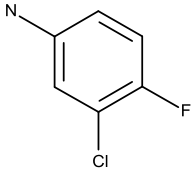	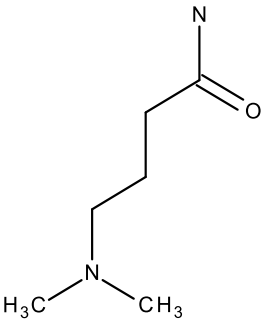	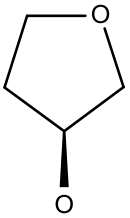	-88.07
Qz89	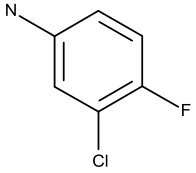	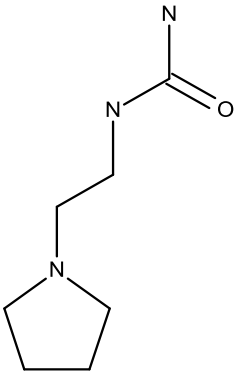	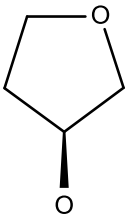	-97.32

Table 2: Docking Score of the highest 10 4,6,7-trisubstituted quinazoline derivatives

Compound number	Chemical structure	Docking score	Amino acid residues forming hydrogen bonds in A0
Qz47	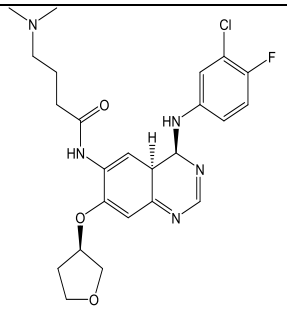	-97.14	Y777 hh -- m M o3: 1.86 Y789 hh -- m M n4: 2.03 E961 hn -- m M o1: 2.11 N784 o -- m M h11: 1.75
Qz60	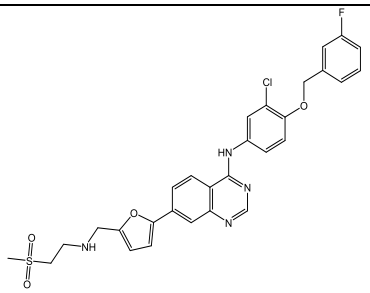	-112.09	R752 he -- m M o3: 2.30 R752 hh21 -- m M o1: 2.32 R752 hh22 -- m M n4: 1.48 R752 hh22 -- m M o3: 2.44 R807 he -- m M n2: 1.84 S744 o -- m M h61: 2.46 Y803 oh -- m M h61: 2.62

Qz66	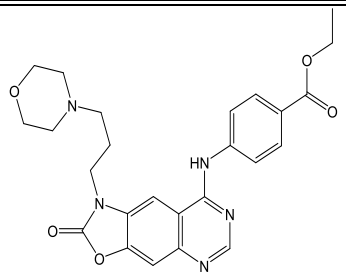	-102.02	K721 hz2 -- m M o4: 1.48 K721 hz3 -- m M o4: 2.27 T766 hg1 -- m M n3: 1.85 M769 hn -- m M n2: 2.46 Q767 o -- m M h131: 1.70
Qz69	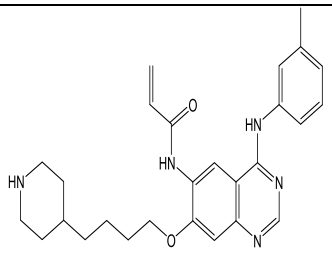	-109.64	M769 hn -- m M n3: 1.82 Q767 o -- m M h91: 1.89
Qz72	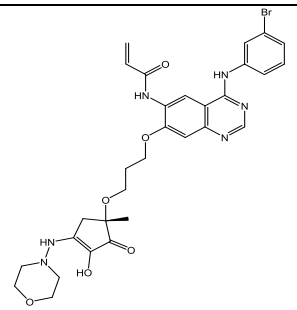	-112.81	K782 hz1 -- m M n2: 1.81 K782 hz2 -- m M n2: 1.76 K782 hz2 -- m M n3: 1.34 K782 hz3 -- m M n2: 2.73 S888 hg -- m M o1: 1.56 K782 o -- m M h02: 1.70 D783 od1 -- m M h61: 2.03 S888 og -- m M h03: 2.12
Qz74	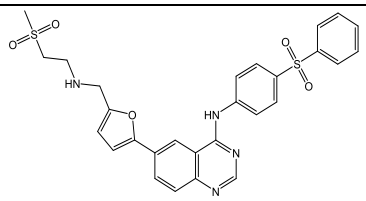	-106.77	Q952 he21 -- m M n4: 1.79 Q952 he21 -- m M o2: 1.06 Q952 he22 -- m M o2: 1.16 Q952 he22 -- m M o3: 1.48 G959 hn -- m M o5: 1.70 N784 od1 -- m M h61: 2.58 D960 od2 -- m M h02: 2.25
Qz83	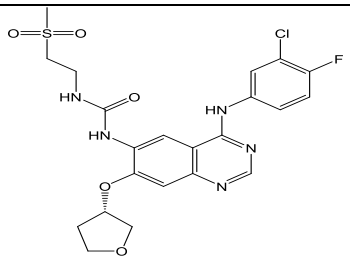	-104.78	I785 hn -- m M o3: 2.66 Q958 hn -- m M o1: 2.62 G959 hn -- m M o2: 2.37 G959 hn -- m M o1: 1.60 D960 hn -- m M o2: 1.53
Qz85	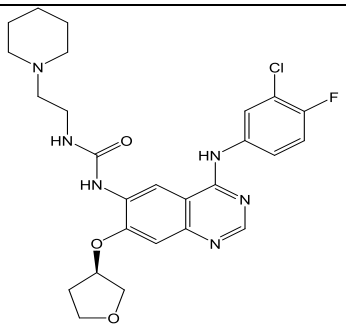	-109.78	K721 hz2 -- m M o1: 1.57 T830 og1 -- m M h11: 2.56 D831 od2 -- m M h11: 2.59 D831 od2 -- m M h21: 2.61

Qz86	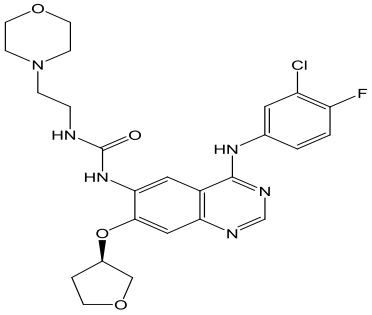	-100.03	Q958 hn -- m M o1: 1.67 D960 hn -- m M o2: 2.37 E961 hn -- m M o2: 1.80 V956 o -- m M h02: 2.03
QZ89	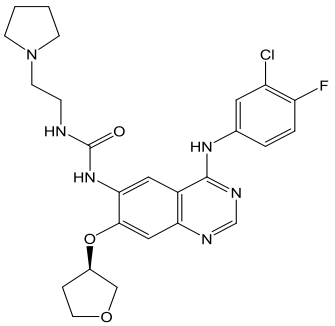	-97.32	D783 hn -- m M n3: 1.88 D783 hn -- m M o1: 2.41 Q958 hn -- m M n5: 2.79 D960 hn -- m M o3: 2.29 E961 hn -- m M o3: 2.31 H781 o -- m M h11: 1.39 K782 o -- m M h11: 2.27 K782 o -- m M h21: 1.34

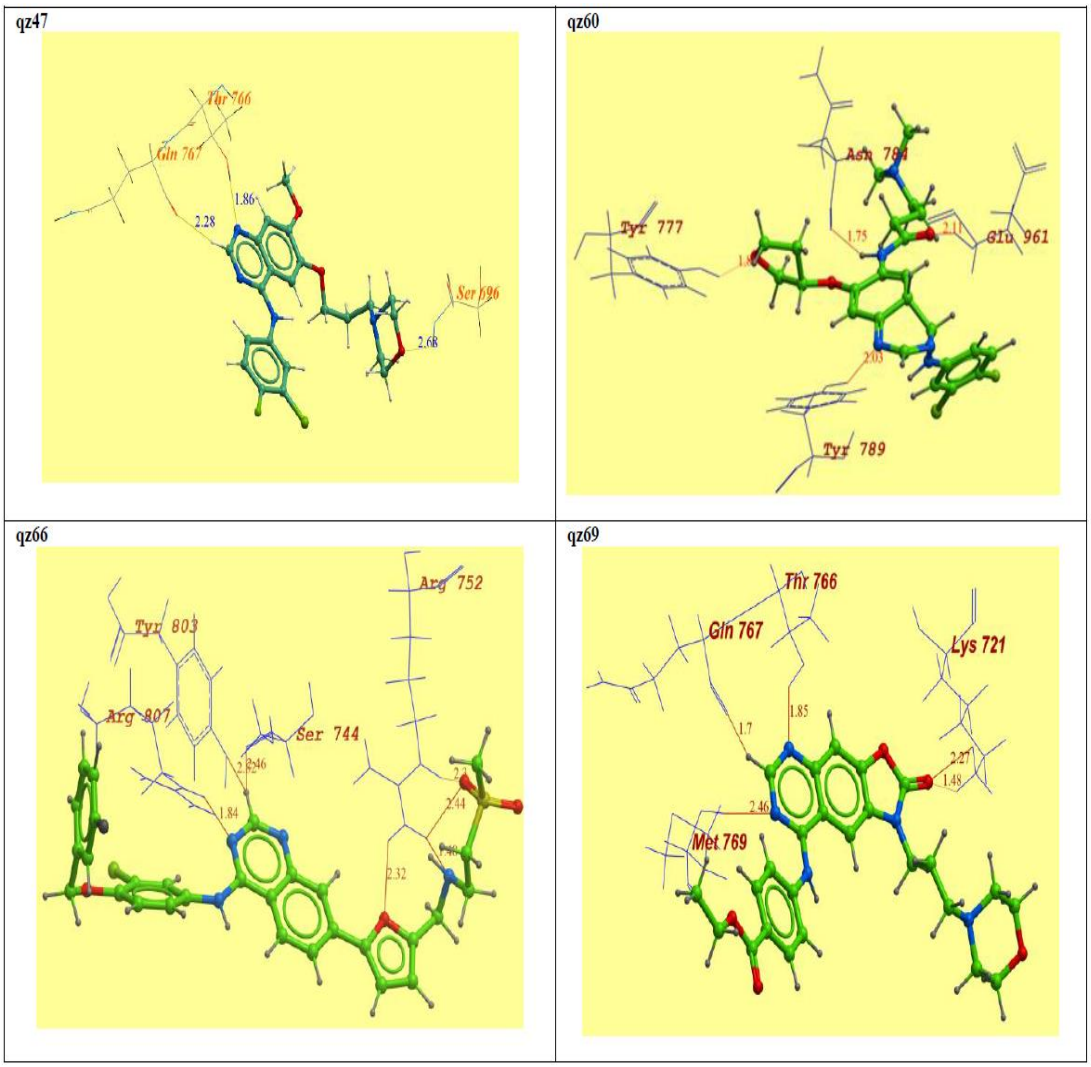

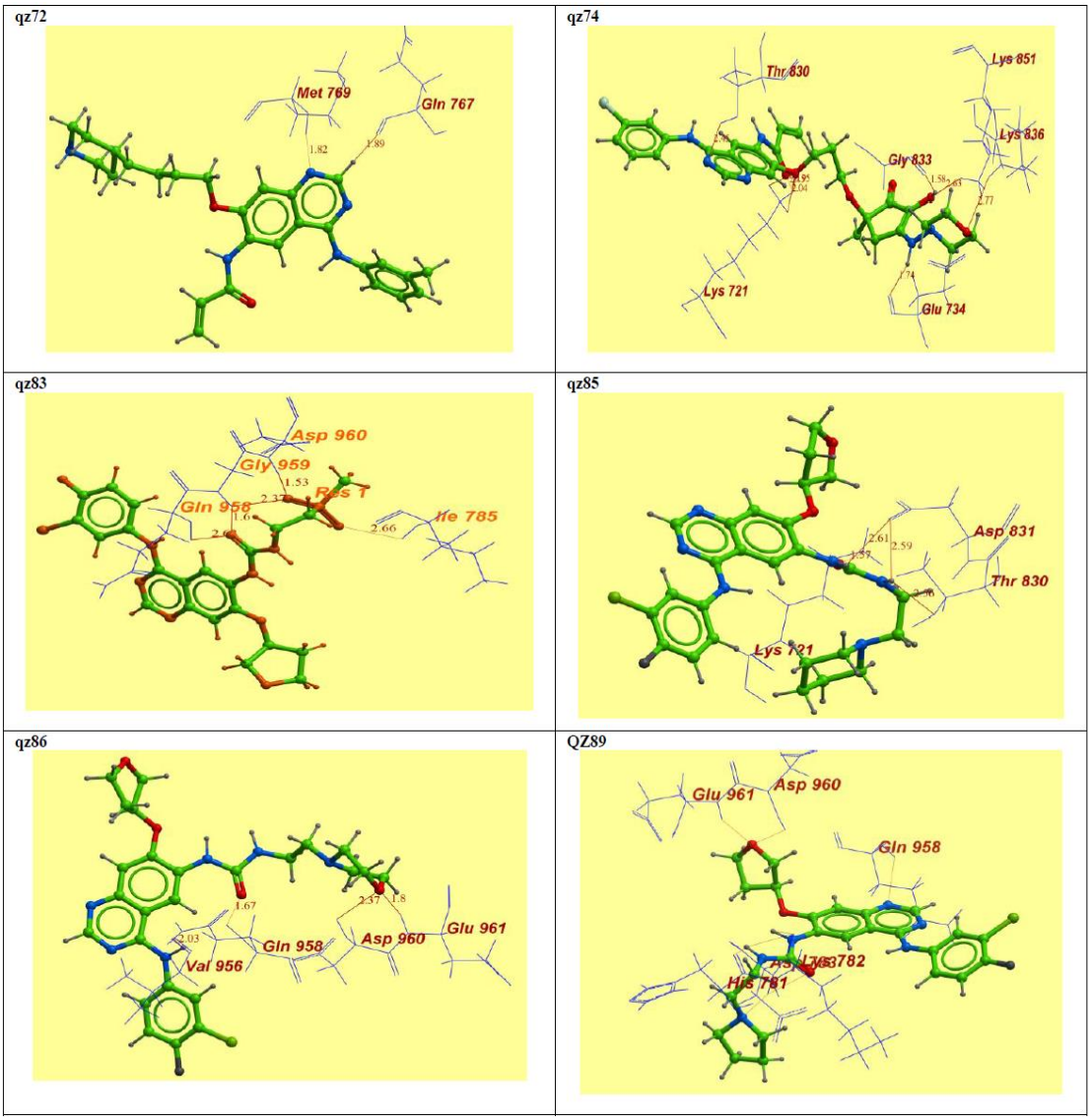

Figure 3: The poses of the highest binding derivatives gefitinib, qz47 qz60, qz66, qz69, qz72, qz74, qz83, qz85, qz86 and QZ89 to the binding site of EGFR

CONCLUSION

Combining the results from this preliminary study with the literature data of EGFR inhibition activity of 4,6,7-resubstituted quinazoline derivatives we can conclude that these compounds are considered as potential anti-cancer drug candidates for its expected EGFR inhibition activity. The presence of N-substituted anilino ring in position 4 of the quinazoline ring is important to enhance the EGFR inhibition activity. On the other hand, regarding the substituents in position 7 of the quinazoline ring, the presence of polar groups or hydrogen bonding acceptor aliphatic groups, O- substituted with small N or O five membered heterocyclic ring is also important to enhance the binding affinity of ligands to the binding site of EGFR.

REFERENCES

[1] H. Naci, A.W. Carter, E. Mossialos, *BMJ*., **2015**, 351.
[2] C.J. Manly, J. Chandrasekhar, J.W. Ochterski, J.D. Hammer, B.B. Warfield, *Drug Discovery Today.*, **2008**, 13(3), 99-109.
[3] A.F. Eweas, I.A. Maghrabi, A.I. Namarneh, *Der Pharma Chemica*., **2014**, 6, 211-228.
[4] J.W. Geldenhuys, **2006**.
[5] A. Baldi, Computational Approaches for Drug Design and Discovery: An Over View, IP: 117.204.64.189, **2010**.
[6] O. Cala, F. Guillière, I. Krimm, Anal. Bioanal. Chem., **2014**, 406(4), 943-956.
[7] M. Calder, S. Gilmore, *Springer Science Business Media*, **2007**, 4695.
[8] L.G. Ferreira, R.N. dos Santos, G. Oliva, A.D. Andricopulo, *Molecules.*, **2015**, 20(7), 13384-13421.
[9] J. Kunes, J. Bazant, M. Pour, K. Waisser, M. Slosarek, J. Janota, *Farmaco.*, **2000**, 55, 725-729.
[10] V. Alagarsamy, V.R. Salomon, G. Vanikavitha, V. Paluchamy, M.R. Chandran, A.A. Sujin, A. Thangathiruppathy, S. Amuthalakshmi, R. Revathi, *Biol. Pharm. Bull*., **2002**, 25(11), 1432-1435.
[11] P.M. Chandrika, Yakaiah, T.B. Narsaiah, *Indian J. Chem.* Section B., **2009**, 48(6), 840-847.

[12] M. Berger, B. Albrecht, A. Berces, P. Ettmayer, W. Neruda, M. Woisetschl, J. Med. Chem., **2001**, 44(18), 3031-3038.
[13] M. Asif, *Int. J Med. Chem*., **2014**.
[14] Tobe, Masanori, *Bioorg. Med. Chem.*, 2003, 609-616.
[15] P.M. Chandrika, T. Yakaiah, B. Narsaiah, V. Sridhar, G. Venugopal, J.V. Rao, A.R.R. Rao, *Indian J. Chem. B*., **2009**, 48, 840-847.
[16] P.M. Chandrika, A.R. Ram Rao, B. Narsaiah, M.B. Raju, *Int. J. Chem. Sci*., **2008**, 6(3), 1119-1146.
[17] A. Motegi, J. Fujimoto, M. Kotani, H. Sakuraba, T. Yamamoto, *J. Cell Sci.*, **2004**, 117(15), 3319-3329.